CALIBRATION OF STEADY-STATE CAR-FOLLOWING MODELS USING MACROSCOPIC LOOP DETECTOR DATA

FINAL REPORT

VT-2008-01
DTRS 99-G-003

Prepared for

Virginia Transportation Research Council

By

Hesham Rakha and Yu Gao

Virginia Tech Transportation Institute

May 2010

VT-2008-01

This work was sponsored by the Virginia Department of Transportation and the U.S. Department of Transportation, Federal Highway Administration.

1. Report No.	2. Government Accession No.	3. Recipient's Catalog No.

4. Title and Subtitle	5. Report Date
CALIBRTION OF STEADY-STATE CAR-FOLLOWING MODELS USING MACROSCOPIC LOOP DETECTOR DATA	May 2010
	6. Performing Organization Code

7. Author(s)	8. Performing Organization Report No.
Hesham Rakha and Yu Gao	VT-2008-01

9. Performing Organization Name and Address	10. Work Unit No. (TRAIS)
Virginia Tech Transportation Institute 3500 Transportation Research Plaza Blacksburg, VA 24061	**11. Contract or Grant No.** DTRS99-G-003

12. Sponsoring Agency Name and Address	13. Type of Report and Period Covered
Virginia Department of Transportation ****** U.S. Department of Transportation Research and Innovative Technology Administration UTC Program, RDT-30 1200 New Jersey Ave., SE Washington, DC 20590	Final Report
	14. Sponsoring Agency Code

15. Supplementary Notes

16. Abstract

The paper develops procedures for calibrating the steady-state component of various car following models using macroscopic loop detector data. The calibration procedures are developed for a number of commercially available microscopic traffic simulation software, including: CORSIM, AIMSUN2, VISSIM, Paramics, and INTEGRATION. The procedures are then applied to a sample dataset for illustration purposes. The paper then compares the various steady-state car-following formulations and concludes that the Gipps and Van Aerde steady-state carfollowing models provide the highest level of flexibility in capturing different driver and roadway characteristics. However, the Van Aerde model, unlike the Gipps model, is a single-regime model and thus is easier to calibrate given that it does not require the segmentation of data into two regimes. The paper finally proposes that the car-following parameters within traffic simulation software be link-specific as opposed to the current practice of coding network-wide parameters. The use of link-specific parameters will offer the opportunity to capture unique roadway characteristics and reflect roadway capacity differences across different roadways.

17. Key Words	18. Distribution Statement
Macroscopic loop detector data, CORSIM, AIMSUN2, VISSIM, Paramics, and INTEGRATION.	No restrictions. This document is available from the National Technical Information Service, Springfield, VA 22161

19. Security Classif. (of this report)	20. Security Classif. (of this page)	21. No. of Pages	22. Price
Unclassified	Unclassified	21	

TABLE OF CONTENTS

LIST OF FIGURES

LIST OF TABLES

ABSTRACT

The paper develops procedures for calibrating the steady-state component of various car-following models using macroscopic loop detector data. The calibration procedures are developed for a number of commercially available microscopic traffic simulation software, including: CORSIM, AIMSUN2, VISSIM, Paramics, and INTEGRATION. The procedures are then applied to a sample dataset for illustration purposes. The paper then compares the various steady-state car-following formulations and concludes that the Gipps and Van Aerde steady-state car-following models provide the highest level of flexibility in capturing different driver and roadway characteristics. However, the Van Aerde model, unlike the Gipps model, is a single-regime model and thus is easier to calibrate given that it does not require the segmentation of data into two regimes. The paper finally proposes that the car-following parameters within traffic simulation software be link-specific as opposed to the current practice of coding network-wide parameters. The use of link-specific parameters will offer the opportunity to capture unique roadway characteristics and reflect roadway capacity differences across different roadways.

INTRODUCTION

The rapid development of personal computers over the last few decades has provided the necessary computing power for advanced traffic micro-simulators. Today, microscopic traffic simulation software are widely accepted and applied in all branches of transportation engineering as an efficient and cost effective analysis tool. One of the main reasons for this popularity is the ability of microscopic traffic simulation software to reflect the dynamic nature of the transportation system in a stochastic fashion.

The core of microscopic traffic simulation software is a car-following model that characterizes the longitudinal motion of vehicles. The process of car-following consists of two levels, namely modeling steady-state and non-steady-state behavior [1]. Ozaki defined steady state as conditions in which the vehicle acceleration and deceleration rate is within a range of ±0.05g [2]. Another definition of steady-state or stationary conditions is provided by Rakha [3] as the conditions when traffic states remain practically constant over a short time and distance. Steady-state car-following is extremely critical to traffic stream modeling given that it influences the overall behavior of the traffic stream. Specifically, it determines the desirable speed of vehicles at different levels of congestion, the roadway capacity, and the spatial extent of queues. Alternatively, non-steady-state conditions govern the behavior of vehicles while moving from one steady state to another through the use of acceleration and deceleration models. The acceleration model is typically a function of the vehicle dynamics while the deceleration model ensures that vehicles maintain a safe relative distance to the preceding vehicle thus ensuring that the traffic stream is asymptotically stable. Both acceleration and deceleration models can affect steady-state conditions by reducing queue discharge saturation flow rates.

Traffic stream models describe the motion of a traffic stream by approximating for the flow of a continuous compressible fluid. The traffic stream models relate three traffic stream measures, namely: flow rate (q), density (k), and space-mean-speed (u). Gazis et al. [4] were the first to derive the bridge between microscopic car-following and macroscopic traffic stream models. Specifically, the flow rate can be expressed as the inverse of the average vehicle time headway. Similarly, the traffic stream density can be approximated for the inverse of the average vehicle spacing for all vehicles within a section of roadway. Therefore every car-following model can be represented by its resulting steady-state traffic stream model. Different graphs relating each pair of the above parameters can be used to show the steady-state properties of a particular

model; including the speed-spacing (*u-s*) and speed-flow-density (*u-q-k*) relationships. The latter curve is of more interest, since it is more sensitive to the calibration process and the shape and nose position of the curve determines the behavior of the resulting traffic stream.

A reliable use of micro-simulation software requires a rigorous calibration effort. Because traffic simulation software are commonly used to estimate macroscopic traffic stream measures, such as average travel time, roadway capacity, and average speed, the state-of-the-practice is to systematically alter the model input parameters to achieve a reasonable match between desired macroscopic model output and field data [5]. Since the macroscopic flow characteristics are mostly related to steady-state conditions, this requires the user to calibrate the parameters of the steady-state relationship and therefore the knowledge of the steady-state behavior of the car-following model is necessary in this process. It should be mentioned that under certain circumstances, the non-steady-state behavior can also influence steady-state behavior [3]; however since this is not the general case, the focus of this paper will be on steady-state conditions.

Over the past decade, several car-following models have been proposed and described in the literature. Brackstone and McDonald [6] categorized the car-following models into five groups, namely: Gazis-Herman-Rothery (GHR) models, safety distance models, linear models, Psycho-physical or action point models, and fuzzy logic based models. However, as it was mentioned above the measures that are usually used by transportation engineers are those of macroscopic nature, which are mostly affected by car-following models. Consequently, calibrating these software using macroscopic data offers a significant appeal to modelers.

The goals of this paper are two-fold. First, the paper identifies the steady-state car-following model for a number of state-of-practice commercial microscopic traffic simulation software. Second, the paper develops a procedure for calibrating these steady-state models using macroscopic loop detector data.

TRAFFIC SIMULATION CAR-FOLLOWING MODELS

The modeling of car-following and traffic stream behavior requires a mathematical representation that captures the most important features of the actual behavior. In this treatment, the relationships obtained by observation, experimentation, and reasoning are given: the researcher attempts to express their steady-state behavior in a graphical form, and classify them based on their steady-state representation.

Typically, car-following models characterize the behavior of a following vehicle (vehicle *n*) that follows a lead vehicle (vehicle *n-1*). This can be presented by either characterizing the relationship between a vehicles' desired speed and the vehicle spacing (speed formulation), or alternatively by describing the relationship between the vehicle's acceleration and speed differential between the lead and following vehicles (acceleration formulation).

Over the last few decades, several car-following models have been developed and incorporated within micro-simulation software packages. This section describes the characteristics of six of the state-of-practice and state-of-art car-following models, including the Pitt model (CORSIM), Gipps' model (AIMSUN2), Wiedemann74 and 99 models (VISSIM), Fritzsche's model (PARAMICS), and the Van Aerde model (INTEGRATION). Subsequently, each model is characterized based on its steady-state behavior and procedures are developed to calibrate the model parameters.

It should be noted again that this study only describes car-following behavior under steady-state conditions, when the lead vehicle is traveling at similar speeds and both the lead and

following having similar car-following behavior, i.e. $s_n \approx s_{desired}$, $\Delta u_n \approx 0$, where s_n.is the spacing between the lead vehicle (vehicle n-1) and following vehicle (vehicle n) and Δu_n is the relative speed between the lead and following vehicle ($u_{n-1} - u_n$). In addition to these two conditions, we are capturing the average behavior given that driver behavior is stochastic in nature. The analysis of randomness was presented in an earlier publication [7] and thus is not considered further in this research effort.

CORSIM Software

CORSIM was developed by the Federal Highway Administration (FHWA) and combines two traffic simulation models: NETSIM for surface streets and FRESIM for freeway roadways. The FRESIM model utilizes the Pitt car-following model that was developed by the University of Pittsburgh [8]. The basic model incorporates the vehicle spacing and speed differential between the lead and following vehicle as two independent variables as demonstrated in Table 1 and cast as

$$s_n(t) = s_j + c_3 \frac{u_n(t+\Delta t)}{3.6} + bc_3 \frac{\Delta u_n (t+\Delta t)^2}{3.6^2}, \quad (1)$$

where $s_n(t)$ is the vehicle spacing between the front bumper of the lead vehicle and front bumper of following vehicle at time t (m), s_j is the vehicle spacing when vehicles are completely stopped in a queue (m), c_3 is the driver sensitivity factor (s), b is a calibration constant that equals 0.1 if the speed of the following vehicle exceeds the speed of the lead vehicle, otherwise it is set to zero (h/km), Δu is the difference in speed between lead and following vehicle (km/h) at instant $t+\Delta t$, and u_n is the speed of the following vehicle at instant t (km/h).

Table 1: Software Car-following Model Formulations

Software	Model	Formulation
CORSIM	Pitt Model	$u_n(t+\Delta t) = \min\left\{3.6\cdot\left[\frac{s_n(t)-s_j}{c_3} - b\left(u_n(t)-u_{n-1}(t)\right)^2\right], u_f\right\}$
VISSIM	Wiedemann74	$u_n(t+\Delta t) = \min\left\{\begin{array}{l} 3.6\cdot\left(\frac{s_n(t)-s_j}{BX}\right)^2 \\ 3.6\cdot\left(\frac{s_n(t)-s_j}{BX\cdot EX}\right)^2 \end{array}, u_f\right\}$
	Wiedemann99	$u_n(t+\Delta t) = \min\left\{\begin{array}{l} u_n(t) + 3.6\cdot\left(CC8 + \frac{CC8-CC9}{80}u_n(t)\right)\Delta t \\ 3.6\cdot\frac{s_n(t)-CC0-L_{n-1}}{u_n(t)} \end{array}, u_f\right\}$
Paramics	Fritzsche	$u_n(t+\Delta t) = \min\left\{\begin{array}{l} 3.6\cdot\left(\frac{AD-A_0}{T_D}\right) \\ 3.6\cdot\left(\frac{AR-A_0}{T_r}\right) \end{array}, u_f\right\}$
AIMSUN2	Gipps	$u_n(t+T) = \min\left\{\begin{array}{l} u_n(t) + 3.6\left[2.5a_{\max}T\left(1-\frac{u_n(t)}{u_f}\right)\sqrt{0.025+\frac{u_n(t)}{u_f}}\right], \\ 3.6\left[-bT + \sqrt{b^2T^2 + b\left(2\left[s_n(t)-L_{n-1}\right] - \frac{u_n(t)}{3.6}T + \frac{u_{n-1}(t)^2}{3.6^2\times b'}\right)}\right] \end{array}\right\}$
INTEGRATION	Van Aerde	$u_n(t+\Delta t) = \min\left\{\begin{array}{l} u_n(t) + 3.6\cdot\frac{F_n(t)-R_n(t)}{m}\Delta t, \\ \frac{-c_1' + c_3u_f + \tilde{s}_n(t) - \sqrt{\left[c_1' - c_3u_f - \tilde{s}_n(t)\right]^2 - 4c_3\left[\tilde{s}_n(t)u_f - c_1'u_f - c_2\right]}}{2c_3} \end{array}\right\}$ Where: $\tilde{s}_n(t) = s_n(t) + \left[u_{n-1}(t+\Delta t) - u_n(t)\right]\Delta t + 0.5a_{n-1}(t+\Delta t)\Delta t^2$

Given that steady-state conditions are characterized by travel at near equal speeds, the third term of the car-following model tends to zero under steady-state driving. Consequently, the steady-state car-following model that is incorporated within FRESIM can be written as

$$s_n(t) = s_j + c_3\frac{u_n(t+\Delta t)}{3.6}. \quad (2)$$

Introducing a constraint on the vehicle speed based on the roadway characteristics and roadway speed limit, the car-following model can be written as

$$u_n(t+\Delta t) = \min\left(u_f, 3.6\left(\frac{s_n(t)-s_j}{c_3}\right)\right). \quad (3)$$

Rakha and Crowther [9] demonstrated that the steady-state car-following behavior is identical to the Pipes or the GM-1 model. Furthermore, if we assume that all vehicles are similar

in behavior, the vehicle subscripts can be dropped from the formulation. The model then requires the calibration of three parameters, namely: the facility free-flow speed, the facility jam density, and a Driver Sensitivity Factor (DSF) c_3. In the case of the NETSIM software the parameter is fixed and equal to 1/3600, however in the case of the FRESIM model Rakha and Crowther [9] showed that the DSF can be related to macroscopic traffic stream parameters as

$$c_3 = 3600\left(\frac{1}{q_c} - \frac{1}{k_j u_f}\right), \quad (4)$$

where q_c is the mean saturation flow rate (veh/h), k_j is the mean roadway jam density (veh/km), and u_f is the space-mean traffic stream free-flow speed (km/h). For example, considering a freeway facility with an average lane capacity of 2400 veh/h/lane, an average free-flow speed of 100 km/h, and an average jam density of 150 veh/km/lane; the DSF can be computed as 1.26 s, as summarized in Table 2. In other words, the modeler would need to input an average DSF of 1.26 s, a free-flow speed of 100 km/h, and an average vehicle spacing of 6.67 m in order to simulate a saturation flow rate of 2400 veh/h/lane. The estimation of the three macroscopic traffic stream parameters q_c, u_f, and k_j using loop detector data is described later in the paper. Rakha and Crowther [9] demonstrated the calibration of the DSF can be achieved by changing a base network-wide parameter and changing link-specific adjustment parameters.

The calibration procedure was applied to a sample arterial dataset in which the traffic stream space-mean speed is sensitive to the flow rate in the uncongested regime, as illustrated in Figure 1. Because the Pipes model assumes that the traffic stream speed remains constant regardless of the flow rate in the uncongested regime the model is not suitable for such applications. Furthermore, the model assumes that the speed-at-capacity is identical to the free-flow speed, which is not the case in this dataset. It should be noted that the capacity for this example is fairly low given that it is measured upstream of a traffic signal.

Table 2: Steady-State Model Calibration

Car-following Model	Steady-State Calibration
Pitt Model	$c_3 = 3600\left(\frac{1}{q_c} - \frac{1}{k_j u_f}\right)$
Wiedemann 74	$E(BX) = 1000\sqrt{3.6}\sqrt{u_f}\left(\frac{1}{\alpha q_c} - \frac{1}{k_j u_f}\right)$ and $E(EX) = \frac{\frac{k_j u_f}{q_c} - 1}{\frac{k_j u_f}{\alpha q_c} - 1} \simeq \alpha$
Wiedemann 99	$CC0 = \frac{1000}{k_j} - \bar{L}$ and $CC1 = 3600\left(\frac{1}{q_c} - \frac{1}{k_j u_f}\right)$
Gipps	b=b′: $T = 2400\left(\frac{1}{q_c} - \frac{1}{k_j u_f}\right)$ b>b′: Invalid behavior with a non-concave car-following relationship b<b′: $b = \frac{1}{\left(\frac{1}{b'} + \frac{25920}{k_j u_c^2}\right)}$ and $T = 2.4\left(\frac{1000}{q_c} - \frac{1000}{k_j u_c} - \frac{u_c}{25.92b}\left(1 - \frac{b}{b'}\right)\right)$
Fritzsche	$A_0 = \frac{1000}{k_j}$; $T_D = 3600\left(\frac{1}{q_c} - \frac{1}{k_j u_f}\right)$; and $T_r = 3600\left(\frac{1}{q_c^{\max}} - \frac{1}{k_j u_f}\right)$
Van Aerde	$c_1 = \frac{u_f}{k_j u_c^2}\left(2u_c - u_f\right)$; $c_2 = \frac{u_f}{k_j u_c^2}\left(u_f - u_c\right)^2$; $c_3 = \left(\frac{1}{q_c} - \frac{u_f}{k_j u_c^2}\right)$

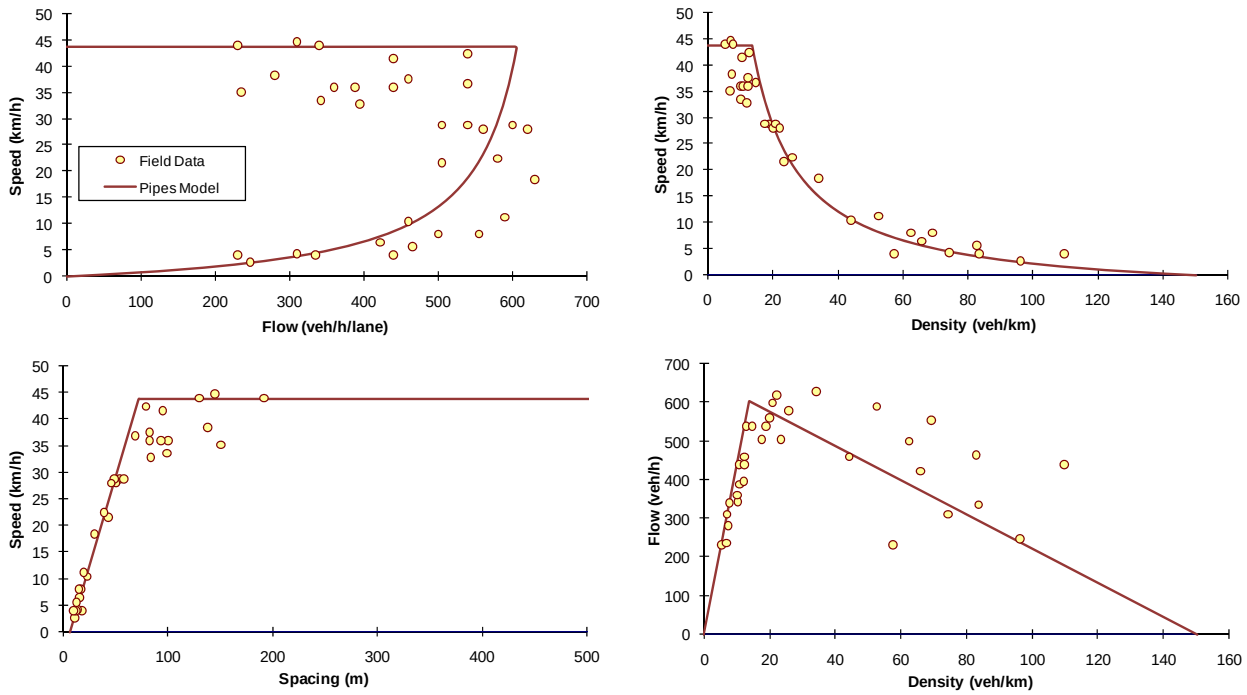

Figure 1: Example Illustration of Pipes Model Calibration

AIMSUN2 Software

The AIMSUN2 car-following behavior is modeled using the Gipps car-following model [10-12] and presented in Table 1. According to Gipps, the speed of the following vehicle is controlled by three conditions. The first condition ensures that the vehicle does not exceed its desired speed or a vehicle-specific free-flow speed (U_n). The second condition ensures that the vehicle accelerates to its desired speed with an acceleration rate that initially increases with speed and then decreases to zero as the vehicle approaches its desired speed. The combination of these conditions results in Equation (5) which controls the vehicle acceleration while vehicles are distant from each other (free-flow behavior). The equation coefficients were obtained from fitting a curve to field data collected on a road of moderate traffic.

$$u_n(t+T) = u_n(t) + 3.6\left[2.5a_nT(1-\frac{u_n(t)}{U_n})\sqrt{0.025+\frac{u_n(t)}{U_n}}\right] \quad (5)$$

where $u_n(t)$ is the speed of vehicle n at time t (km/h); a_n is the maximum desired acceleration rate of vehicle n (m/s^2); T it the driver's reaction time (s); and U_n is the desired speed of vehicle n or the vehicle-specific free-flow speed (km/h).

In a constrained traffic situation, when vehicles are traveling close to each other, the third condition becomes dominant and controls the behavior of the follower vehicle while decelerating. The speed of the follower vehicle (see Equation (6)) is affected by the driver reaction time, the spacing between the leader and follower vehicles, the speed of the leader and follower vehicles, and the deceleration rates they are willing to employ. Gipps pointed out that a safety margin should be added to the driver's reaction time. The safety margin would assure the vehicle's ability to stop even when there is a delay to initiate its reaction for some reason. The safety margin was assumed to be constant in value and equal to $T/2$ (half the reaction time). This safety value is implicit in Equation (6).

$$u_n(t+T) = 3.6\left[-bT + \sqrt{b^2T^2 + b\left\{2\left[s_n(t) - L_{n-1}\right] - \frac{u_n(t)}{3.6}T + \frac{u_{n-1}(t)^2}{3.6^2 \times b'}\right\}}\right] \quad (6)$$

Here b and b' are deceleration parameters of vehicle n (m/s^2); b is the actual most severe deceleration rate the vehicle is willing to employ in order to avoid a collision; and b' is the estimated most severe deceleration rate the leader vehicle is willing to employ. It is an estimated value because it is impossible for the follower to evaluate the real intention of his/her leader; L_{n-1} is the effective length of vehicle n-1 (the actual length plus a safety margin); $s_n(t)$ is the spacing between vehicle n and n-1 at time t (m); and $u_{n-1}(t)$ is the speed of the preceding vehicle (km/h).

The parameters related to deceleration rates (b and b') are very important for the braking process modeling. These parameters influence the spacing between the follower and leader vehicles and thus affect the lane capacity.

Assuming the vehicles will travel as close to their desired speed as possible and considering the dynamics limitations, the speed of vehicle n at time $t+T$ can be computed as

$$u_n(t+T) = \min\left\{\begin{array}{l} u_n(t) + 3.6\left[2.5a_{\max}T\left(1 - \frac{u_n(t)}{u_f}\right)\sqrt{0.025 + \frac{u_n(t)}{u_f}}\right], \\ 3.6\left[-bT + \sqrt{b^2T^2 + b\left(2\left[s_n(t) - L_{n-1}\right] - \frac{u_n(t)}{3.6}T + \frac{u_{n-1}(t)^2}{3.6^2 \times b'}\right)}\right] \end{array}\right\} \quad (7)$$

According to the above formulation, once the road is unconstrained and the space headways between the vehicles are large enough to allow them to travel at their desired speed, the first argument of Equation (7) is applied. In this case, the following vehicle is able to accelerate according to the empirical equation of vehicle dynamics. Alternatively, in congested conditions, where short headways are typical, the second argument of Equation (7) is applied. In such a case, the speed is limited by the leader vehicle performance. Each vehicle establishes its speed in order to avoid a collision based on the assumption that the leader deceleration rate will not exceed b'.

A detailed mathematical analysis of Gipps' car-following model under steady-state conditions was presented in two earlier publications [11, 12]. Consequently, the paper will only summarize the major findings of these studies and then develop an analytical calibration procedure of the model. In his study, Wilson [12] presented a mathematical analysis of simplified scenarios and identified parameter regimes that deserve further investigation. The paper also showed the derivation of uniform flow solutions (steady-state) and speed-spacing functions under simplifying conditions concerning parameters b, b', and T, and an analysis of the linear stability of the uniform flow, identifying stable and non-stable flow regimes. Wilson demonstrated that the steady-state car-following model can be cast as

$$s = s_j + \frac{1}{2.4}Tu + \frac{1}{25.92\,b}\left(1 - \frac{b}{b'}\right)u^2. \quad (8)$$

Rakha et al. [11] demonstrated that in the case that b and b' are identical the driver reaction time can be computed as

$$T = 2400\left(\frac{1}{q_c} - \frac{1}{k_j u_f}\right). \quad (9)$$

When b is set greater than b', Wilson [12] demonstrated that the car-following relationship may become unphysical and produce multiple solutions for some sets of parameters.

Consequently, b should be set less than or equal to b'. In the case that b is less than b', Rakha et al. [11] demonstrated that the steady-state car-following relationship can be cast as

$$u = \min\left(u_f, \frac{5.4bT}{\left(1-\frac{b}{b'}\right)}\left[-1+\sqrt{1+\frac{8000\left(\frac{1}{k}-\frac{1}{k_j}\right)\left(1-\frac{b}{b'}\right)}{9bT^2}}\right]\right). \quad (10)$$

Starting with Equation (8) the speed-flow relationship can be derived as

$$q = \frac{1000u}{s_j + \frac{1}{2.4}Tu + \frac{1}{25.92\,b}\left(1-\frac{b}{b'}\right)u^2}. \quad (11)$$

Using the function of Equation (11) Rakha et al. developed lookup tables to estimate the facility capacity considering different microscopic car-following parameters. This paper extends the research by developing analytical expressions to estimate the microscopic car-following model parameters based on macroscopic traffic stream measurements.

Considering that the maximum flow rate occurs when the first derivative of flow with respect to speed equals to zero, the speed-at-capacity can be computed as

$$u_c = \min\left(3.6\times\sqrt{\frac{2000b}{k_j\left(1-\frac{b}{b'}\right)}}, u_f\right). \quad (12)$$

Consequently, we derive the relationship between the microscopic car-following and macroscopic traffic stream parameters as

$$b = \frac{1}{\left(\frac{1}{b'}+\frac{25920}{k_j u_c^2}\right)} \text{ where } b < b', \text{ and} \quad (13)$$

$$T = 2.4\left(\frac{1000}{q_c}-\frac{1000}{k_j u_c}-\frac{u_c}{25.92b}\left(1-\frac{b}{b'}\right)\right). \quad (14)$$

The calibration of the model entails assuming the most severe deceleration rate the driver is willing to employ (b') and then computing b using Equation (13) for a desired facility-specific mean speed-at-capacity and jam density. The reaction time (T) can then be computed using Equation (14), as demonstrated in Table 2. It should be noted that in the case that b=b' Equation (14) reverts to Equation (9) given that the speed-at-capacity equals the free-flow speed as computed using Equation (12).

The calibration procedure was applied to the same sample dataset gathered along an arterial, as illustrated in Figure 2. The figure demonstrates a reasonable fit to the data, however given that the data demonstrate that traffic stream speed is sensitive to the traffic stream flow in the uncongested regime; the model offers a sub-optimal fit to the field data for the uncongested regime with a good fit for the congested regime. The speed-at-capacity is different from the free-flow speed and thus the model is able to capture this phenomenon.

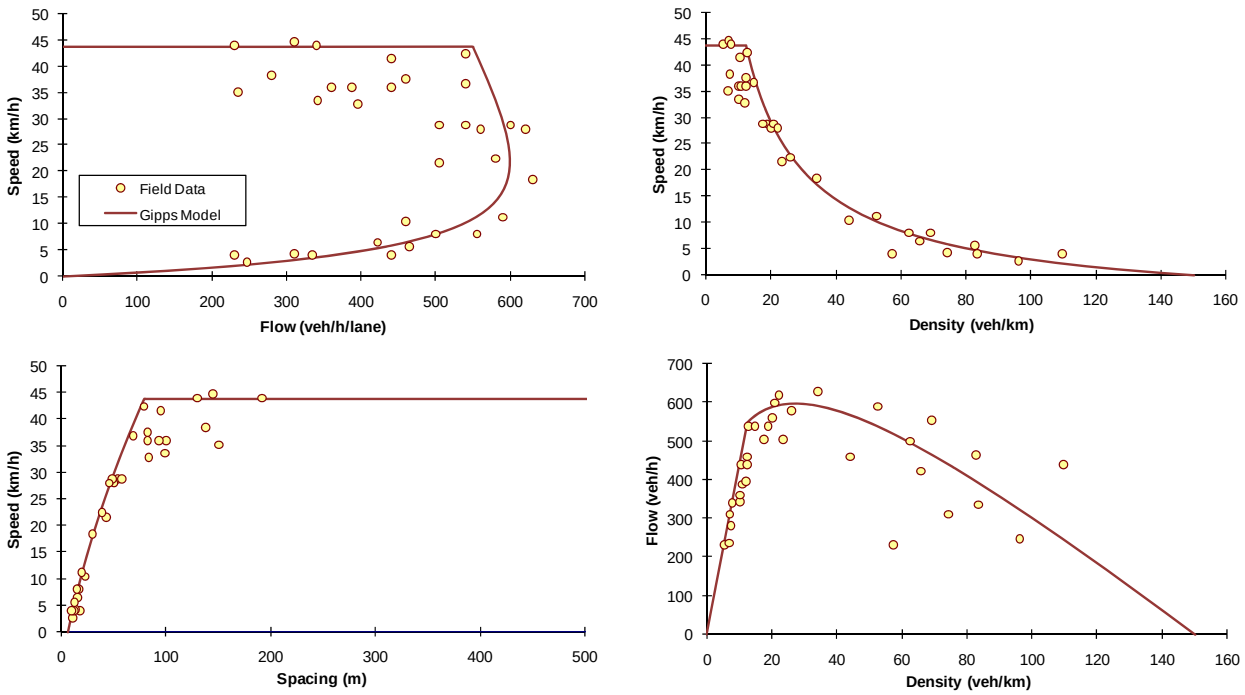

Figure 2: Example Illustration of Gipps Model Calibration

VISSIM Software

The car-following model used in VISSIM is a modified version of two models developed by Wiedemann (Wiedemann74 and 99 models) and belongs to a family of models known as psychophysical or action-point models. This family of models uses thresholds or action-points where the driver changes his/her driving behavior. Drivers react to changes in spacing or relative speed only when these thresholds are crossed. The thresholds and the regimes they define are usually presented in the relative speed/spacing diagram for a pair of lead and follower vehicles.

First the Wiedemann74 model is described followed by a description of the Wiedemann99 model. For the purposes of this study only the area identified as steady-state is of interest. This area as was mentioned before has the following steady-state criteria ($s_n \approx s_{desired}$, $\Delta u_n \approx 0$). In the case of the Wiedemann74 model, the desired vehicle spacing is an interval ($ABX \le s \le SDX$) instead of a single value as was the case with previously mentioned models. Given that $\Delta u_n \approx 0$, only the boundaries of desired vehicle spacing interval (*ABX* & *SDX*) determine the steady-state characteristics of the VISSIM car-following model. The expected value of *ABX* and *SDX* parameters can be calculated as

$$E(AX) = s_j + AXadd + AXmult \cdot E(RND1_n) = s_j + 0.5 \approx s_j, \quad (15)$$

$$E(ABX) = E(AX) + E(BX)\sqrt{u} = s_j + E(BX)\sqrt{u}, \qquad u \le u_{desired}, \text{ and} \quad (16)$$

$$E(SDX) = s_j + E(BX) \cdot E(EX)\sqrt{u}, \qquad u \le u_{desired}. \quad (17)$$

Where the *BX* and *EX* random variables are computed as

$$BX = BXadd + BXmult \cdot RND1_n, \text{ and} \quad (18)$$

$$EX = EXadd + BXmult \cdot (NRND - RND2_n). \quad (19)$$

Here $RND1_n$ and $RND2_n$ are user specified vehicle-specific (where n is the vehicle index) normally distributed random variables with a default mean value of 0.5 and a standard deviation of 0.15. *NRND* is also a normally distributed random variable with a default mean value of 0.5 and standard deviation of 0.15. The expectation of *SDX* given as E(*SDX*) ranges between 1.5 to 2.5 times the expected value of *ABX* (E(*ABX*)), where BX_{add}, BX_{mult} , EX_{add}, and EX_{mult} are user-defined calibration parameters.

Equations (16) and (17) demonstrate that the parameters *ABX* and *SDX* are not internally constrained and thus an external maximum speed constraint ($u \le u_{desired}$) must be enforced. Given that the desired speed is insensitive to traffic conditions ($u_{desired} = u_c = u_f$), the uncongested steady-state behavior has a flat top, as illustrated in Figure 3.

In order to calibrate the steady-state Wiedemann74 model the following calibration procedure is developed. The calibration of the Wiedemann74 model can be achieved by deriving the speed-flow relationship for the congested regime as

$$q = \frac{1000u}{\frac{1000}{k_j} + \frac{E(BX)E(EX)}{\sqrt{3.6}}\sqrt{u}}. \tag{20}$$

Here u is the traffic stream space-mean speed (km/h); q is the traffic stream flow rate (veh/h), and k_j is the traffic stream density (veh/km). By taking the derivative of flow with respect to speed the relationship is demonstrated to be a strict monotonically increasing function as shown in Equation (21).

$$\frac{dq}{du} = \frac{1000\left(\frac{1000}{k_j} + \frac{E(BX)\cdot E(EX)}{2\cdot\sqrt{3.6}}\sqrt{u}\right)}{\left(\frac{1000}{k_j} + \frac{E(BX)\cdot E(EX)}{\sqrt{3.6}}\sqrt{u}\right)^2} > 0 \tag{21}$$

Consequently, the maximum flow occurs at the boundary of the relationship and thus at the maximum desired or free-flow speed. As was the case with the Pipes' model, the speed-at-capacity equals the free-flow speed. By inputting the maximum flow (capacity) and free-flow speed in Equation (20), removing the E(*EX*) term to compute the capacity upper bound, and re-arranging the equation; the expected value of *BX* can be computed as

$$E(BX) = 1000\sqrt{3.6}\sqrt{u_f}\left(\frac{1}{\alpha q_c} - \frac{1}{k_j u_f}\right). \tag{22}$$

By considering that the expected value of *SDX* is α times the expected value of *ABX* (i.e. E(*SDX*) = α × E(*ABX*)), where the parameter α ranges from 1.5 to 2.5; the expected value of *EX* can be computed as

$$E(EX) = \frac{\frac{k_j u_f}{q_c} - 1}{\frac{k_j u_f}{\alpha q_c} - 1} \simeq \alpha \tag{23}$$

Given that $k_j u_f / q_c$ is typically very large, the expected value of *EX* is approximately equal to the parameter α.

The proposed calibration procedure was applied to the same arterial dataset and the fit is illustrated in Figure 3. Again, as was the case with the Pipes' model the fit to the field data is

unable to reflect the reduction is traffic stream speed as the arrival rate increases in the uncongested regime. Furthermore, the curvature of the car-following model (speed-spacing diagram) contradicts typical driver behavior (curvature is convex instead of concave). The model does provide a range of behavior for the congested regime as illustrated by the two lines.

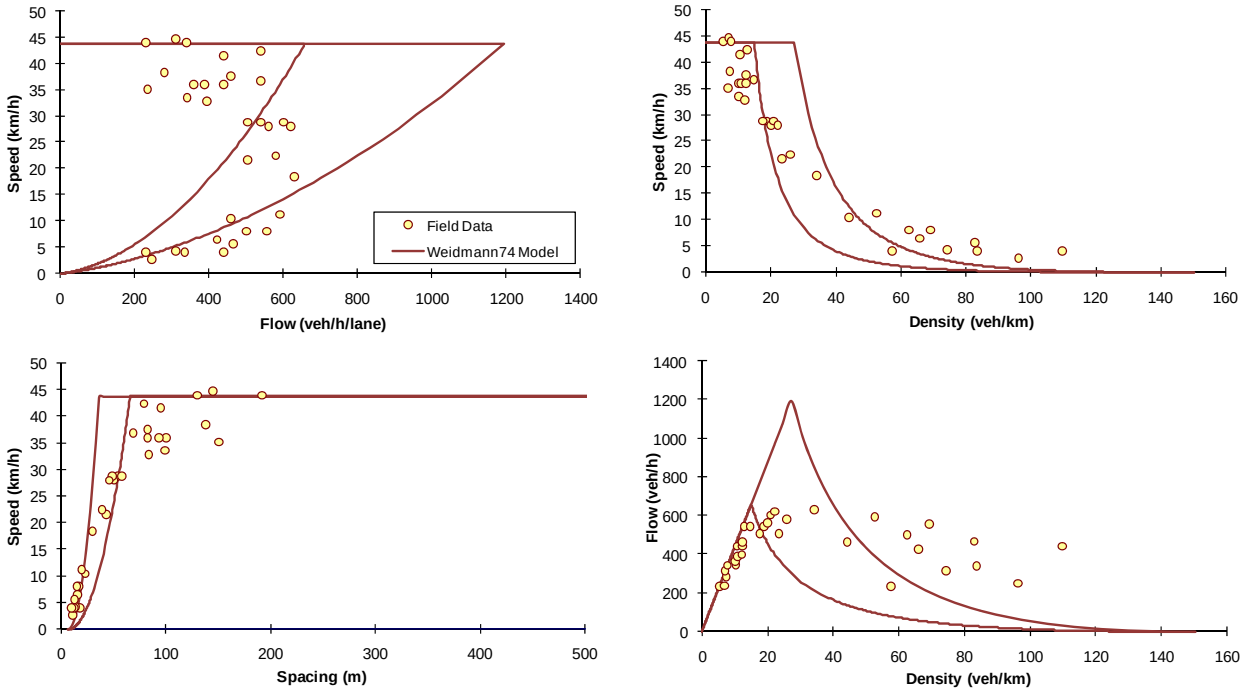

Figure 3: Sample Calibration of the Wiedemann74 Model

In an attempt to validate the calibration procedure a simple network was coded and simulated using the VISSIM software. The network was composed of two single-lane links in order to isolate the car-following behavior (i.e. remove any possible impact that lane-changing behavior might have on the traffic stream performance). Initially the capacity of both links was set equal using the proposed calibration procedure. The arrival rate was increased gradually until it exceeded the capacity of the entrance link. The traffic stream flow and speed were measured using a number of loop detectors along the first link. The default model randomness was set (AXadd = 2, BXadd = 3, and BXmult = 4). The results demonstrate that the uncongested regime is flat as was suggested earlier, as illustrated in Figure 4. Subsequently, the capacity at the downstream link was reduced by selecting the input parameters using the calibration procedures presented earlier. The demand was fixed at the capacity of the upstream link and thus a bottleneck was created at the entrance to link 2. The departure flow rate and speed were directly measured upstream of the bottleneck to construct the congested regime of the fundamental diagram. As demonstrated in Figure 4 the simulated data appear to initially follow the ABX curve and then move towards the *SDX* curve as the capacity of the downstream bottleneck increases. Given that the movement between the two regimes is not documented in the literature it is not clear how this is done. The figure clearly demonstrates that the proposed calibration procedures are consistent with the VISSIM model output.

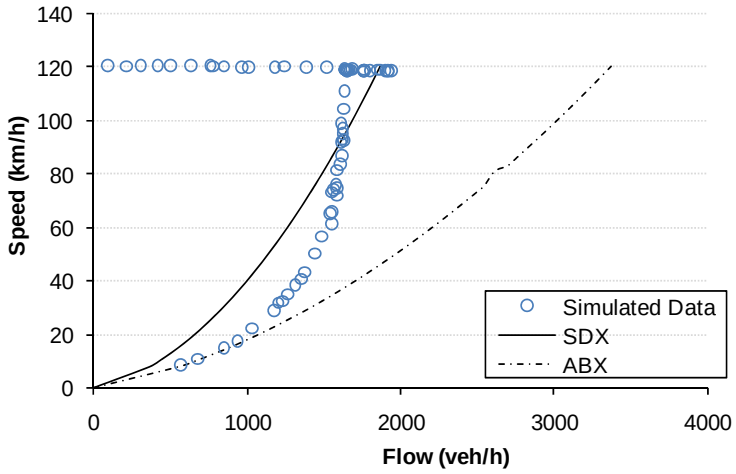

Figure 4: Wiedemann74 Calibration Procedure Validation

The VISSIM software also offers a second car-following model, namely the Wiedemann99 model. The model is formulated as

$$u_n(t+\Delta t) = \min\left\{\begin{array}{l} u_n(t) + 3.6\cdot\left(CC8 + \dfrac{CC8 - CC9}{80}u_n\left(t\right)\right)\Delta t \\ 3.6\cdot\dfrac{s_n(t) - CC0 - L_{n-1}}{u_n(t)} \end{array}, u_f\right\}. \quad (24)$$

This model, as was the case with the Gipps model, computes the vehicle speed as the minimum of two speeds: one based on the vehicle acceleration restrictions and the other based on a steady-state car-following model. The model considers a vehicle kinematics model with a linear speed-acceleration relationship where *CC8* is the maximum vehicle acceleration at a speed of 0 km/h (m/s^2) and *CC9* is the maximum vehicle acceleration at a speed of 80 km/h (m/s^2). The VISSIM software also allows the user to input a user-specified vehicle kinematics model that appears to over-ride the linear model. This user specified relationship allows the user to modify the desired and maximum driver speed-acceleration relationship. The second term of Equation (24) computes the vehicle's desired speed using a linear car-following model and thus is identical to the Pipes model.

Consequently, as was done with the Pipes model the model constants *CC0* and *CC1* (also known as the Driver Sensitivity Factor) can be computed as

$$CC0 = \frac{1000}{k_j} - \bar{L}\text{, and} \quad (25)$$

$$CC1 = 3600\left(\frac{1}{q_c} - \frac{1}{k_j u_f}\right). \quad (26)$$

Where *CC0* is the spacing between the front bumper of the subject vehicle and the rear bumper of the lead vehicle. This equals the jam density spacing minus the average vehicle length. The Driver Sensitivity Factor (*CC1*) can be calibrated using three macroscopic traffic stream parameters, namely: the expected roadway capacity, jam density, and free-flow speed.

Paramics Software

The car-following model utilized in the Paramics software, as was the case with the VISSIM software, is a psychophysical car-following model that was developed by Fritzsche [13]. Fritzsche's model uses the same modeling concept as the Wiedemann74 car-following model. The difference between these two models is the way thresholds are defined and calculated. Figure 5 depicts the Fritzsche model's thresholds in the $\Delta u - \Delta x$ plane.

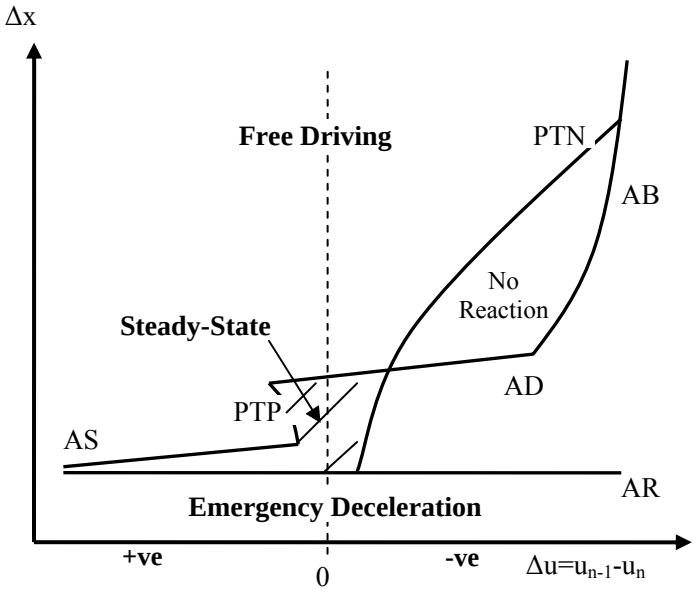

Figure 5: Fritzsche's Car-following Model: a) Thresholds and Regimes, b) and c) Steady-state Behavior

The area corresponding to steady-state conditions is almost identical to Wiedemann's car-following model. The vehicle spacing for this regime lies between the desired spacing (*AD*) and the risky spacing (*AR*). These two boundaries are determined as

$$AR = A_0 + T_r \times \frac{u_n}{3.6}, \text{ and} \tag{27}$$

$$AD = A_0 + T_D \times \frac{u_{n-1}}{3.6}. \tag{28}$$

Where A_0 is the vehicle spacing at jam density, T_r is the risky time gap (usually 0.5 s), T_D is the desired time gap (with a recommended value of 1.8 s). The resulting steady-state car-following model can be written as

$$u_n(t+\Delta t) = \min\left\{\begin{matrix} 3.6 \cdot \left(\frac{AD - A_0}{T_D}\right) \\ 3.6 \cdot \left(\frac{AR - A_0}{T_r}\right) \end{matrix}, u_f\right\}$$

Similar to the Wiedemann car-following model, the desired speed constraint must be enforced externally. Again, as was the case with the Wiedemann74 model the relationship provides a range of car-following behavior within the congested regime. Unlike the

Wiedemann74 model the car-following model is linear and thus a Pipes model. Using similar calibration procedures, the various car-following model parameters are related to macroscopic traffic stream parameters as

$$A_0 = \frac{1000}{k_j}; \tag{29}$$

$$T_D = 3600\left(\frac{1}{q_c} - \frac{1}{k_j u_f}\right); \text{ and} \tag{30}$$

$$T_r = 3600\left(\frac{1}{q_c^{\max}} - \frac{1}{k_j u_f}\right). \tag{31}$$

The calibration procedure was applied to the same arterial dataset and the results are similar to those of the Wiedemann74 model, as illustrated in Figure 6. It should be noted that the car-following model provides a range of data in the congested regime considering a linear car-following modeling.

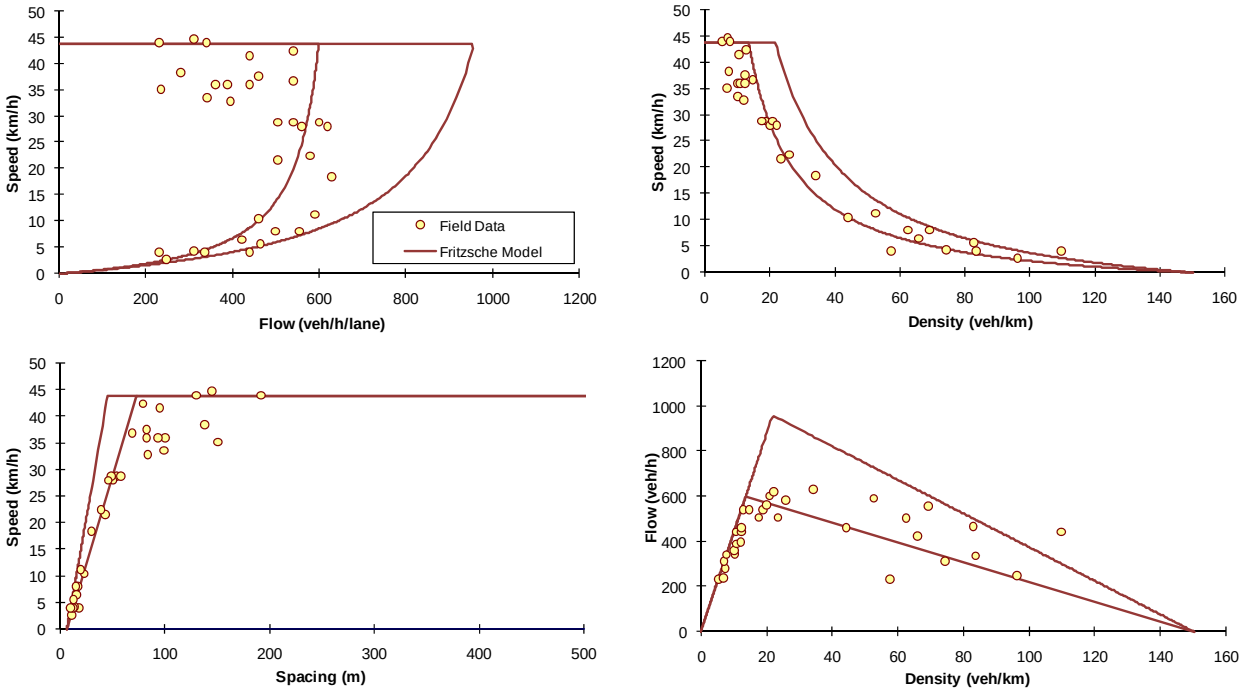

Figure 6: Sample Calibration of the Fritzsche Model

INTEGRATION Software

The steady-state functional form that is utilized in the INTEGRATION software is the Van Aerde nonlinear functional form that was proposed by Van Aerde [14] and Van Aerde and Rakha [15], which is formulated as

$$s_n(t) = c_1 + c_3 u_n(t+\Delta t) + \frac{c_2}{u_f - u_n(t+\Delta t)}, \tag{32}$$

where c_1, c_2, and c_3 are model constants. Demarchi [16] demonstrated that by considering three boundary conditions the model constants can be computed as

$$c_1 = \frac{u_f}{k_j u_c^2}\left(2u_c - u_f\right); \quad c_2 = \frac{u_f}{k_j u_c^2}\left(u_f - u_c\right)^2; \quad c_3 = \left(\frac{1}{q_c} - \frac{u_f}{k_j u_c^2}\right). \qquad [33]$$

As was demonstrated by Rakha and Crowther [17] this functional form amalgamates the Greenshields and Pipes car-following models.

Ignoring differences in vehicle behavior within a traffic stream and considering the relationship between traffic stream density and traffic spacing, the speed-density relationship can be derived as

$$k = \frac{1000}{c_1 + \frac{c_2}{u_f - u} + c_3 u}, \qquad [34]$$

Of interest is the fact that Equation [34] reverts to Greenshields' linear model, when the speed-at-capacity and density-at-capacity are both set equal to half the free-flow speed and jam density, respectively (i.e. $u_c=u_f/2$ and $k_c=k_j/2$). Alternatively, setting $u_c=u_f$ results in the linear Pipes model given that

$$c_1 = \frac{1}{k_j} = s_j; \quad c_2 = 0; \quad c_3 = \frac{1}{q_c} - \frac{1}{k_j u_f}.$$

Rakha [3] demonstrated that the wave speed at jam density (denoted as w_j) can be computed by differentiating the speed-density relationship with respect to density at jam density, to be

$$w_j = k_j \left.\frac{du}{dk}\right|_{k_j} = -s_j \left.\frac{du}{ds}\right|_{s_j}. \qquad [35]$$

By applying Equation [32] to [34] and ignoring differences between vehicles Rakha derived

$$w_j = -s_j \left.\frac{1}{\frac{ds}{du}}\right|_{u=0} = -\frac{s_j}{c_3 + \frac{c_2}{u_f^2}} = -\frac{u_f}{k_j\left(c_3 u_f^2 + c_2\right)} = -\left[\left(\frac{k_j}{q_c} - \frac{u_f}{u_c^2}\right) + \frac{\left(u_f - u_c\right)^2}{u_f u_c^2}\right]^{-1}. \qquad [36]$$

Considering, a typical lane capacity of 2400 veh/h, a free-flow speed of 110 km/h (which is typical of US highways), and a jam density of 140 veh/km/lane, the wave velocity at jam density ranges between approximately -11.5 to -20.3 km/h, when the speed-at-capacity is varied from 80 to 100% the free-flow speed (which is typical on North American freeways).

As was demonstrated earlier, the Van Aerde model reverts to the Pipes linear model when the speed-at-capacity is set equal to the free-flow speed. Consequently, it can be demonstrated that under this condition the wave speed of [36] reverts to

$$w = -\frac{q_c u_f}{k_j u_f - q_c}, \qquad [37]$$

which is the speed of the linear model. Furthermore, when $u_c=u_f/2$ and $k_c=k_j/2$ the wave speed at jam density is consistent with the Greenshields model estimates and is computed as

$$w_j = -u_f. \qquad [38]$$

Field observations demonstrate a concave speed-headway relationship. Consequently, the derivative of the speed-density relationship was computed as

$$\frac{du}{ds} = \frac{1}{c_3 + \frac{c_2}{\left(u_f - u\right)^2}} = \frac{\left(u_f - u\right)^2}{c_3\left(u_f - u\right)^2 + c_2}. \quad [39]$$

Given that the c_2, c_3, and u_f parameters are always positive, [3] demonstrated the function is a strictly increasing monotonic function. Alternatively, the speed-density relationship is a strictly decreasing monotonic function as

$$\frac{du}{dk} = \frac{du}{ds} \cdot \frac{ds}{dk} = -\frac{\left(u_f - u\right)^2}{c_3\left(u_f - u\right)^2 + c_2} \cdot \frac{1}{k^2}. \quad [40]$$

While a strict monotonic function is desired from a theoretical stand point, it is not necessarily reflective of real-life driving behavior. For example drivers might abide by a facility speed limit if they are the only vehicle on a roadway, however if other vehicles are present on the roadway slower drivers might be encouraged to follow faster vehicles recognizing the lower likelihood of being ticketed for over-speeding. This behavior may only hold when the traffic stream density is very low but contradicts typical traffic flow theory.

The Van Aerde model was calibrated to the same arterial data that were presented earlier, as illustrated in Figure 7. The figure demonstrates that the model is extremely flexible and thus is capable of providing a good fit to the field data for the entire range of data both in the uncongested and congested regimes. It should be noted that the fit provides the expected relationship. Differences in driver behavior can be captured by introducing differences in the four traffic stream parameters, namely: free-flow speed, speed-at-capacity, capacity, and jam density.

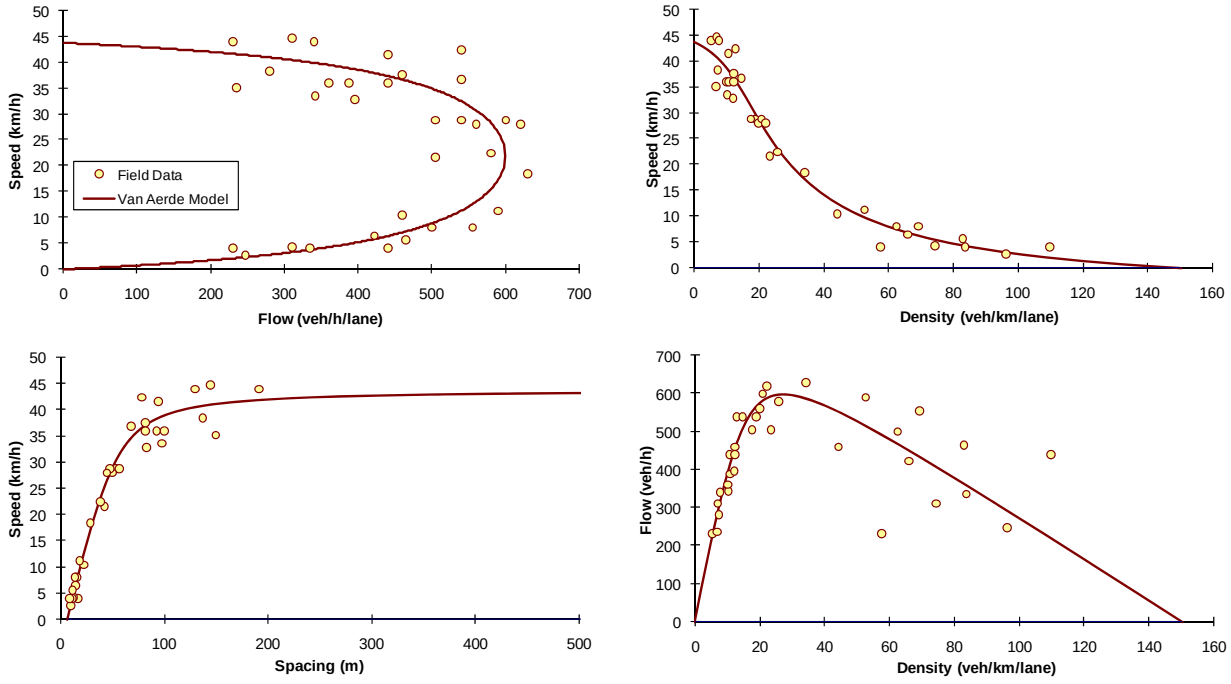

Figure 7: Sample Calibration of the Van Aerde Model

TRAFFIC STREAM MODEL CALIBRATION

The estimation of the four traffic stream parameters (u_f, u_c, q_c, and k_j) requires the calibration of a traffic stream model to loop detector data. This effort entails making four decisions, namely: (1) define the functional form to be calibrated, (2) identify the dependent and the independent variables, (3) define the *optimum* set of parameters, and (4) develop an optimization technique to compute the set of parameter values. Van Aerde and Rakha [15] and later Rakha and Arafeh [18] developed a calibration approach that minimizes the orthogonal error about the 3-D fundamental diagram to estimate the expected value of the four traffic stream parameters. The model is briefly described here, however a more detailed description is provided elsewhere [18]. The approach is unique because it does not require the identification of dependent and independent variables since it applies a neutral regression approach (minimizes the orthogonal error).

If we consider the Van Aerde functional form given that it provides the highest level of flexibility, as was demonstrated in the previous section, the optimization model can be formulated as

$$\text{Min} \qquad E = \sum_i \left\{ \left(\frac{u_i - \hat{u}_i}{\tilde{u}} \right)^2 + \left(\frac{q_i - \hat{q}_i}{\tilde{q}} \right)^2 + \left(\frac{k_i - \hat{k}_i}{\tilde{k}} \right)^2 \right\}. \tag{41}$$

S.T.

$$\begin{aligned}
&\hat{k}_i = \frac{1}{c_1 + \dfrac{c_2}{u_f - \hat{u}_i} + c_3 \hat{u}_i} && \forall i \\
&\hat{q}_i = \hat{k}_i \times \hat{u}_i && \forall i \\
&\hat{q}_i, \hat{k}_i, \hat{u}_i \geq 0 && \forall i \\
&\hat{u}_i < u_f && \forall i \\
&0.5u_f \leq u_c \leq u_f; \quad q_c \leq \frac{k_j u_f u_c}{2u_f - u_c} \\
&c_1 = \frac{u_f}{k_j u_c^2}\left(2u_c - u_f\right); \quad c_2 = \frac{u_f}{k_j u_c^2}\left(u_f - u_c\right)^2; \quad c_3 = \frac{1}{q_c} - \frac{u_f}{k_j u_c^2} \\
&u_f^{\min} \leq u_f \leq u_f^{\max};\ u_c^{\min} \leq u_c \leq u_c^{\max};\ q_c^{\min} \leq q_c \leq q_c^{\max};\ k_j^{\min} \leq k_j \leq k_j^{\max}
\end{aligned} \tag{42}$$

Where u_i, k_i, and q_i are the field observed space-mean speed, density, and flow measurements, respectively. The speed, density, and flow variables with hats (^) are estimated speeds, densities, and flows while the tilde variables (~) are the maximum field observed speed, density, and flow measurements. All other variables are defined as was done earlier in describing the Van Aerde functional form.

The objective function ensures that the formulation minimizes the normalized orthogonal error between the three-dimensional field observations and the functional relationship – in this case the Van Aerde functional form. The three error terms are normalized in order to ensure that the objective function is not biased towards reducing the error in one of the three variables at the expense of the other two variables. This data normalization ensures that the parameters in each of the three axes range from 0.0 to 1.0 and thus a minimization of the orthogonal error provides a quality of fit that is equivalent across all three axes.

The initial set of constraints, which is non-linear, ensures that the Van Aerde functional form is maintained, while the second set of constraints is added to constrain the third dimension, namely the flow rate. The third and fourth set of constraints guarantees that the results of the minimization formulation are feasible. The fifth set of constraints, ensures that the four parameters that are selected do not result in any inflection points in the speed-density relationship (i.e. it ensures that the density at any point is less than or equal to the jam density). A detailed derivation of the final constraint is provided elsewhere [3]. The sixth set of equations provides estimates for the three model constants based on the roadway's *mean* free-flow speed (u_f), speed-at-capacity (u_c), capacity (q_c), and jam density (k_j). The final set of constraints provides a valid search window for the four traffic stream parameters that are being optimized (u_f, u_c, q_c, and k_j).

The total number of independent decision variables equals twofold the number of field observations plus the four traffic stream parameters u_f, u_c, q_c, and k_j. For example a problem with 100 observations results in a total of 204 independent decision variables (2x100 + 4). The heuristic approach that was developed earlier was applied to the data to estimate the four traffic stream parameters [15, 18]. Once the four traffic stream parameters are estimated the individual car-following models can be calibrated using the equations provided in Table 2.

CONCLUSIONS

The paper developed procedures for calibrating the steady-state component of various car-following models using macroscopic loop detector data. The paper then compared the various steady-state car-following formulations and demonstrated that the Gipps and Van Aerde steady-state car-following models provide the highest level of flexibility in capturing different driver and roadway characteristics. However, the Van Aerde model, unlike the Gipps model, is a single-regime model and thus is easier to calibrate given that it does not require the segmentation of data into two regimes. An analysis of existing software demonstrated that a number of car-following parameters are network- and not link-specific and thus do not offer model users with the flexibility of coding different roadway capacities for different facility types. In some software, however, arterial and freeway roadway car-following parameters can be coded separately, as in the case of CORSIM and VISSIM. However, major roadway capacity differences can be observed within the broad range of facility categories. For example the saturation flow rate may vary from 1300 to 2000 veh/h on an arterial depending on the roadway and driver characteristics. Consequently, the paper recommends that modifications be made to the various software to allow more flexibility in setting link-specific car-following parameters.

ACKNOWLEDGEMENT

The authors acknowledge the valuable input from Dr. William Perez of Cambridge Systematics, Inc. and Roemer Alfelor and David Yang of the Federal Highway Administration. Finally, the authors acknowledge the financial support provided by the FHWA and the Mid-Atlantic University Transportation Center (MAUTC) in conducting this research effort.

REFERENCES

1. Rakha, H., P. Pasumarthy, and S. Adjerid. *The INTEGRATION framework for modeling longitudinal vehicle motion*. in *TRANSTEC*. 2004. Athens, Greece.
2. Ozaki, H., *Reaction and Anticipation in the Car-following Behavior*, in *12th International Symposium on Transportation and Traffic Theory*. 1993, Elsevier. p. 349-366.

3. Rakha, H.A. *Validation of Van Aerde's simplified steady-state car-following and traffic stream model*. in *85th Transportation Research Board Annual Meeting*. 2006. Washington D.C.: Transportation Research Board.
4. Gazis, D., R. Herman, and R. Rothery, *Nonlinear follow-the-lead models of traffic flow*. Operations Research, 1961. **9(4)**: p. 545-567.
5. Dowling, R., et al., *Guideline for Calibration of Micro-simulation Models: Framework and Applications.* Transportation Research Record, 2004. **1876**: p. 1-9.
6. Brackstone, M. and M. McDonald, *Car-following: a historical review.* Transportation Research, 1999. **2F**: p. 181-196.
7. Farzaneh, M. and H. Rakha, *Impact of differences in driver desired speed on steady-state traffic stream behavior.* Transportation Research Record: Journal of the Transportation Research Board, 2006. **1965**: p. 142-151.
8. Halati, A., H. Lieu, and S. Walker, *CORSIM- Corridor Traffic Simulation Model* in *76th Transportation Research Board Meeting*. 1997: Washington DC.
9. Rakha, H. and B. Crowther, *Comparison and calibration of FRESIM and INTEGRATION steady-state car-following behavior.* Transportation Research, 2003. **37A**: p. 1-27.
10. Gipps, P.G., *A behavioral car-following model for computer simulation.* Transportation Research, 1981. **15B**: p. 105-111.
11. Rakha, H., C.C. Pecker, and H.B.B. Cybis. *Calibration procedure for the Gipps' car-following model*. in *86th Transportation Research Board Annual Meeting*. 2007. Washington, DC: Transportation Research Board.
12. Wilson, R.E., *An analysis of Gipps' car-following model of highway traffic.* IMA Journal of Applied Mathematics, 2001. **66**: p. 509-537.
13. Fritzsche, H.T., *A model for traffic simulation.* Traffic Engineering and Control, 1994. **5**: p. 317-321.
14. Van Aerde, M., *Single regime speed-flow-density relationship for congested and uncongested highways.* Presented at the 74th TRB Annual Conference, Washington DC, Paper No. 950802., 1995.
15. Van Aerde, M. and H. Rakha. *Multivariate calibration of single regime speed-flow-density relationships*. in *Proceedings of the 6th 1995 Vehicle Navigation and Information Systems Conference*. 1995. Seattle, WA, USA: Vehicle Navigation and Information Systems Conference (VNIS) 1995. IEEE, Piscataway, NJ, USA,95CH35776..
16. Demarchi, S.H. *A new formulation for Van Aerde's speed-flow-density relationship. (in portuguese)*. in *XVI Congresso De Pequisa e Ensino em Transportes*. 2002. Natal, RN, Brazil.
17. Rakha, H. and B. Crowther, *Comparison of Greenshields, Pipes, and Van Aerde car-following and traffic stream models.* Transportation Research Record. , 2002(1802): p. 248-262
18. Rakha, H. and M. Arafeh. *Tool for calibrating steady-state traffic stream and car-following models*. in *Transportation Research Board Annual Meeting*. 2007. Washington, D.C.: TRB.